PHYSICAL REVIEW C VOLUME 16, NUMBER 6 DECEMBER 1977

Quasimolecular states in the ^{12}C-^{12}C system*

Jae Y. Park
Physics Department, North Carolina State University, Raleigh, North Carolina 27607

Walter Greiner
Institut für Theoretische Physik der Universität, Frankfurt am Main, Germany

Werner Scheid
Institut für Theoretische Physik der Universität, Giessen, Germany

(Received 31 May 1977)

Quasimolecular resonance structures in the ^{12}C-^{12}C system are studied in the framework of the coupled channel formalism in the energy range $E_{c.m.} = 5$–14 MeV. The influence of the coupling of the first excited 2^+ state in ^{12}C on the resonance structures is investigated by choosing various types of coupling potentials. The intermediate structures in the reflection and transition coefficients and cross sections can be interpreted with the double resonance mechanism.

[NUCLEAR REACTIONS $^{12}C(^{12}C, ^{12}C)$, quasimolecular states, coupling potentials, coupled channel calculations for $\sigma(\theta)$.]

I. INTRODUCTION

In 1960 structure of nonstatistical origin in the ^{12}C-^{12}C cross section near the Coulomb barrier was discovered by Bromley *et al.*,[1,2] who first introduced the concept of nuclear molecular states. The resonances observed were explained by Bromley *et al.*,[1] Vogt and McManus,[3] and Davis[4] as states in a quasimolecular potential. Considerably later, resonances below the Coulomb barrier were observed by Patterson *et al.*,[5] Mazarakis and Stephens,[6] and Spinka and Winkler.[7] Recently, Erb *et al.*,[8] looking for the transitions to low-lying states of ^{20}Ne, have found resonance states at $E_{c.m.} = 7.71$ and 9.84 MeV in the $^{12}C(^{12}, \alpha)$-$^{20}Ne^*$ reaction. This same reaction and the reaction $^{12}C(^{12}C, p)^{23}Na^*$ were measured by Basrak *et al.*,[9] who detected several resonances in the energy range $E_{c.m.} = 7$–10 MeV. Both reactions were also investigated by Voit *et al.*,[10,11] and the reaction $^{12}C(^{12}C, p)^{23}Na^*$ by Cosman *et al.*[12] who summarized the known resonances as a rotational band of quasimolecular states in the ^{24}Mg system. Fletcher *et al.*[13] and Eberhard *et al.*[14] could identify resonances in the reaction $^{12}C(^{12}C, ^8Be)^{16}O$ between $E_{c.m.} = 11$–20 MeV. Further recent experimental results on resonances are listed in Refs. 2, 15–17, and 37.

Davis[4] was one of the first to suggest that the intermediate structure in the ^{12}C-^{12}C elastic excitation function may be due to resonances in a quasimolecular nucleus-nucleus potential. He assumed that the quasimolecular states can be excited directly. An indirect excitation of the potential states via the inelastic excitation of the first excited ^{12}C state at 4.43 MeV was proposed by Imanishi[18] to explain the resonance states near the Coulomb barrier. In Ref. 19, Scheid, Greiner, and Lemmer have introduced the double resonance mechanism in order to interpret the intermediate structure of the excitation function above the Coulomb barrier as caused by the inelastic excitation of quasibound states in the molecular potential well. In the double resonance model the elastic and inelastic partial waves of the relative nucleus-nucleus motion resonate simultaneously with their corresponding virtual and quasibound molecular potential states. In that process a sufficiently large transition strength is generated to create intermediate structure in the excitation function. This structure, with widths of 0.1–0.5 MeV, is superimposed over the gross structure (widths of 2 MeV) which is due to the direct excitation of virtual potential states.

In Ref. 20 Park, Scheid, and Greiner have found a molecular-type adiabatic potential for the ^{12}C-^{12}C system. The quasibound states of this potential reproduce some of the prominent resonances observed in the total reaction cross section and γ-ray yield of the ^{12}C-^{12}C reaction at sub-Coulomb barrier energies. Similar interpretations of the resonance structures in the ^{12}C-^{16}O system were made earlier by Nagorcka and Newton.[21] In this paper we apply the potential of Ref. 20, which was adapted to the sub-Coulomb ^{12}C-^{12}C resonances, for the explanation of the resonances above the Coulomb barrier up to $E_{c.m.} = 14$ MeV. As shown by Fink, Scheid, and Greiner[22] the coupling of the first excited 2^+ state in ^{12}C leads to intermediate structure above the Coulomb barrier in the cross

sections. Therefore, in this paper we also couple the first excited 2^+ state to the elastic channel and obtain intermediate structure in the cross sections at energies at which the conditions for the double resonance effect are fulfilled.

Similar calculations were done by Kondo, Matsuse, and Abe[23] who solved the coupled equations by a variational method, assuming the inelastic channels as closed channels, so that their calculated results (especially widths) are not certain at higher energies. Coupled channel calculations for $E_{\text{c.m.}} \geq 20$ MeV have recently been carried out by Tanimura,[24] who stresses the importance of the mutual excitation of the ^{12}C nuclei at these energies.

The aim of this paper is to study systematically the effects of the coupling on the reflection and transition coefficients. In Secs. II and III we discuss the model applied for the ^{12}C-^{12}C scattering and various possible methods for deriving coupling potentials. The analysis of the reflection and transition coefficients and their interpretation in the framework of the double resonance mechanism is given in Sec. IV. Finally, in Sec. V we compare and analyze the obtained results with the experimentally observed cross sections and resonances.

II. COUPLED EQUATIONS

The scattering and inelastic excitation of two identical nuclei, e.g., ^{12}C nuclei, is described by the following Hamiltonian[22]:

$$H = T(\vec{r}) + W(\vec{r}, 1, 2) + H_0(1) + H_0(2) . \tag{1}$$

The Hamiltonian consists of the kinetic energy T of the relative motion, of the interaction W between the two nuclei (where 1 and 2 abbreviate the coordinates for the intrinsic degrees of freedom of the individual nuclei), and of the intrinsic Hamiltonians H_0 of the separated nuclei. The interaction between the nuclei can be divided up into the average optical potential $U(r)$, depending on the internuclear distance only, and into multipole potentials which couple the intrinsic degrees of freedom with the relative motion:

$$W(\vec{r}, 1, 2) = U(r) + \sum_{L,M} Q_{LM}(r, 1, 2) Y^*_{LM}(\vartheta, \varphi) . \tag{2}$$

The scattering problem $H\psi = E\psi$ is solved with channel wave functions expressed in the eigenstates of the separated nuclei:

$$\varphi_{I_1 I_2 JM}(1, 2) = \frac{1}{[2(1+\delta_{I_1 I_2})]^{1/2}} \times [\chi_{I_1}(1) \otimes \chi_{I_2}(2) + (-)^I \chi_{I_1}(2) \otimes \chi_{I_2}(1)]^{[J]}_M \tag{3a}$$

with the eigensolutions χ_{IM} of $H_0(i)$:

$$H_0(i)\chi_{IM}(i) = \epsilon_I \chi_{IM}(i) . \tag{3b}$$

Here, we have characterized the levels of the separated nuclei simply by their spin since we restrict further consideration only to the ground state and the first 2^+ state in ^{12}C. The scattering wave functions, having total angular momentum I and projection M, are given by

$$\psi_{IM} = \sum_{l I_1 I_2 J} R^I_{l I_1 I_2 J}(r) [i^l Y_l \otimes \varphi_{I_1 I_2 J}(1, 2)]^{[J]}_M . \tag{4}$$

The radial functions solve the system of coupled differential equations[22]:

$$\left[-\frac{\hbar^2}{2\mu r^2}\frac{d}{dr} r^2 \frac{d}{dr} + U(r) + \frac{l(l+1)\hbar^2}{2\mu r^2} + \epsilon_{I_1} + \epsilon_{I_2} - E\right] R^I_{l I_1 I_2 J}(r) = -\sum_{l' I_1' I_2' J' L} i^{l'-l}(-)^{l'+I+J} \begin{Bmatrix} I & J & l \\ L & l' & J' \end{Bmatrix} (l \| Y_L \| l')(I_1 I_2 J \| Q_L \| I_1' I_2' J') R^I_{l' I_1' I_2' J'}(r) . \tag{5}$$

The asymptotic form of the relative wave function can be expressed with ingoing and outgoing Coulomb functions J, O and the S matrix elements $S^I_{KK_0}$:

$$R^I_{l I_1 I_2 J}(r) = J_K(r)\delta_{KK_0} - O_K(r) S^I_{KK_0} , \qquad K = (l I_1 I_2 J) . \tag{6}$$

When only the single excitation of ^{12}C to the first 2^+ state is considered, we have two coupled channels for $I = 0$ and four coupled channels for $I = 2, 4, \ldots$ with the channel quantum numbers:

$$l = I, \quad I_1 = 0, \quad I_2 = 0, \quad J = 0 ; \qquad l = I-2, I, I+2, \quad I_1 = 2, \quad I_2 = 0, \quad J = 2 . \tag{7}$$

The calculation of the S matrix elements and the formulas for the differential cross sections are discussed in great detail in Ref. 22.

III. POTENTIALS

A. Optical potential

The direct potential $U(r)$ in Eq. (2) consists of a real and imaginary part. The real part of the $^{12}C + ^{12}C$ potential is taken from Ref. 20 and was determined there by fitting the position and spacing of the observed sub-Coulomb resonances in the total cross section. In that procedure the real potential was varied between the limiting case of an adiabatic and a sudden potential. As shown in

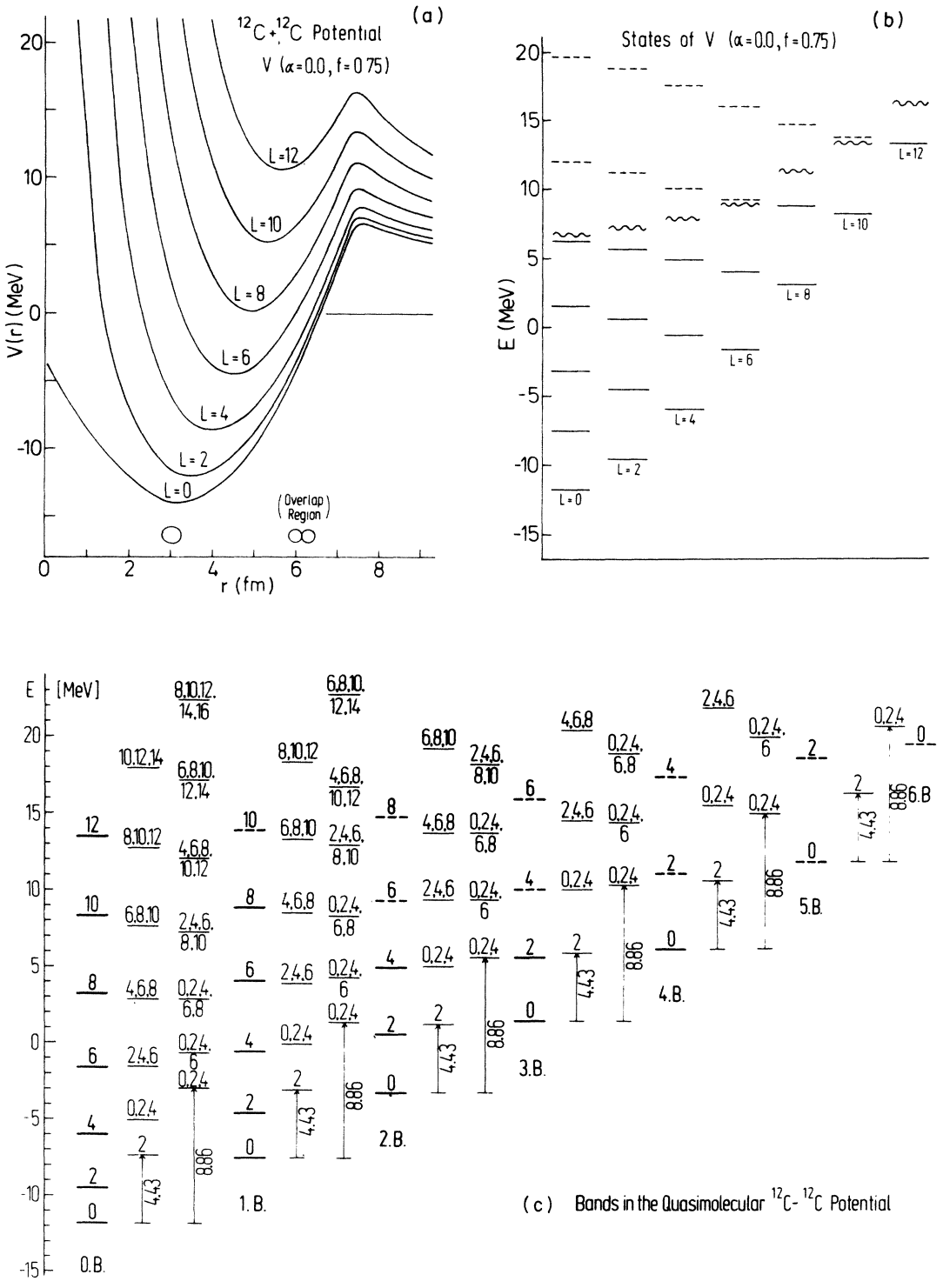

FIG. 1. (a) Effective quasimolecular ^{12}C-^{12}C potential from Ref. 20. The centrifugal potentials are added for even angular momenta. (b) Bound, quasibound (full lines), and virtual (dashed lines) states in this potential. The positions of the corresponding Coulomb barriers are shown by wavy lines. (c) The resonance states arranged in rotational bands. The resonance states of the quasimolecular potential without intrinsic excitation are drawn by heavy lines. The states with the single and simultaneous excitation of the 2^+ (4.43 MeV) state in ^{12}C are degenerate as indicated by their angular momenta. The states are listed in Table I.

Fig. 1(a) the real potential is an adiabatic potential of molecular type with a potential minimum of −14 MeV at $r = 3$ fm. The bound and quasibound states (solid lines) and virtual states (dashed lines) of the potential are presented in Fig. 1(b).

The imaginary part of the optical potential $U(r)$ is chosen the same as in Ref. 20 and has Woods-Saxon form with surface absorption:

$$W(r) = \frac{W_0 \exp[(r-b)/a]}{(1+\exp[(r-b)/a])^2} . \tag{8}$$

The parameters are taken as $a = 0.6$ fm and $b = 2(12)^{1/3} r_0$ ($r_0 = 1.35$ fm), whereas W_0 is varied. The strength W_0 can be set to zero in the inelastic channels to simulate an angular-momentum-dependent imaginary potential. The idea behind that procedure is discussed in Refs. 22 and 25. The gross and intermediate structures in the cross sections of $^{12}C + ^{12}C$, $^{12}C + ^{16}O$, and $^{16}O + ^{16}O$ are caused by grazing partial waves which resonate nearly unabsorbed with the resonances in the quasimolecular nucleus-nucleus potential. These quasimolecular resonance states, with high angular momenta, lie near the yrast line of the compound system and, therefore, have only a small overlap with the states of the compound nucleus. Since the inelastic channels are mainly excited via the grazing partial waves, the inelastic partial waves feel only a small absorption potential which can be set to zero in first approximation.

B. Coupling potentials

The coupling potentials in Eqs. (2) depend sensitively on models for the scattering process and are not so well known as the direct potential $U(r)$. Since the transition potentials are functions of the intrinsic coordinates of the two colliding nuclei, we assume that the intrinsic structure of the ^{12}C nuclei can be described by multipole deformation coordinates $\alpha_{lm}^{(1,2)}$ of their density distributions and shapes. For separated nuclei the nuclear density distributions and shapes are given by

$$\begin{aligned} &\rho_i(\vec{r}_i) = \rho(r_i) + \sum_{l,m} \alpha_{lm}^{(i)} \rho_l(r_i) Y_{lm}^*(\Omega_i) , \\ &R^i(\Omega_i) = R\left(1 + \sum_{l,m} \alpha_{lm}^{(i)} Y_{lm}^*(\Omega_i)\right) , \\ &i = 1, 2 . \end{aligned} \tag{9}$$

The coordinates r_i, Ω_i are measured with respect to the centers of the nuclei $i = 1, 2$. R is the spherical radius.

The transition potentials depend strongly on the nuclear density distribution and shape of the overlapping nuclei. Various methods may be used in order to extrapolate the definition of the multipole deformation coordinates into the interaction region. The simplest method is the folding procedure in which the densities of the nuclei are added up in the interaction region. In that case, which we denote as sudden approach, the asymptotic definition of the multipole coordinates can be kept also in the interaction region.[22] In the adiabatic approach the definition of the multipole coordinates has to be taken as r-dependent as pointed out in Ref. 26.

Independent of the definition of the multipole coordinates in the interaction region, the transition potential in Eq. (2) can be expanded in powers of the multipole deformation coordinates. Up to second order we find the general form for identical nuclei:

$$\begin{aligned} Q_{LM}(r,1,2) = I_L(r)[(-)^L \alpha_{LM}^{(1)} + \alpha_{LM}^{(2)}] + \sum_{L_1 \le L_2} J_{L_1 L_2 L}(r)[(\alpha_{L_1}^{(1)} \otimes \alpha_{L_2}^{(1)})_M^{[L]} + (-)^L (\alpha_{L_1}^{(2)} \otimes \alpha_{L_2}^{(2)})_M^{[L]}] \\ + K_{L_1 L_2 L}(r)[(\alpha_{L_1}^{(1)} \otimes \alpha_{L_2}^{(2)})_M^{[L]} + (-)^L (\alpha_{L_1}^{(2)} \otimes \alpha_{L_2}^{(1)})_M^{[L]}] . \end{aligned} \tag{10}$$

Since the interaction potential in Eq. (1) vanishes asymptotically, the transition potentials I_L, $J_{L_1 L_2 L}$, and $K_{L_1 L_2 L}$ approach zero for large internuclear separations. The matrix elements of Q_L in Eq. (5) contain the reduced matrix elements $(I_1 \| \alpha_l \| I_2)$ of the multipole coordinates which can be related to the experimental electromagnetic transition probabilities or calculated in the framework of nuclear model, e.g., by applying the rotator model for ^{12}C in Ref. 18. In our calculations, where we study the excitation of the first 2^+ state in ^{12}C, we only take the transition matrix element to the first 2^+ state into account using the following relation with the experimental $B(E2)$ value:

$$|\langle \text{g.s.} \| \alpha_2 \| 2^+ \rangle|^2 = 5\left(\frac{4\pi}{3ZeR^2}\right)^2 B(E2, 2^+ \to \text{g.s.}) \tag{11}$$

with $B[E2, 2^+(4.43\ \text{MeV}) \to \text{g.s.}] = 8.453\ e^2\,\text{fm}^4$ from Ref. 27.

The diagonal reduced matrix element $\langle 2^+ \| \alpha_2 \| 2^+ \rangle$ measures the quadrupole moment of the first 2^+ state and is not included in the present calculations. It would lead to additional diagonal potentials in the inelastic channels in the coupled equations (5) with the effect that the undisturbed potential resonances would have different positions in

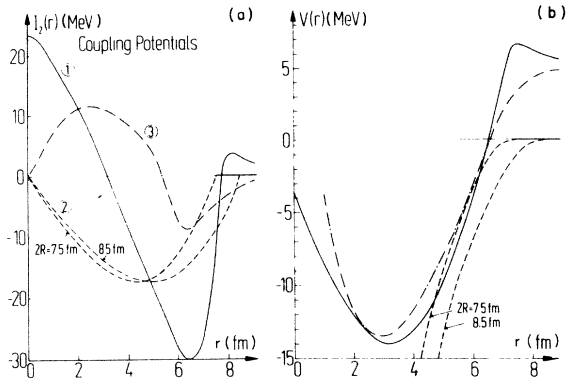

FIG. 2. (a) Radial dependence of three different types of the coupling potentials. The coupling potential (1) (full line) is the derivative form of the real potential $V(r)$ of Fig. 1(a). The coupling potential (2) corresponds to a δ force between the two ^{12}C nuclei with strength $\alpha = -60$ MeV and $2R = 7.5$ and 8.5 fm (dashed lines). The corresponding real potential is shown in Fig. 2(b). The coupling potential (3) is calculated with the two-body potential given in Eq. (15) which is composed of two terms of Yukawa form with $V_1 = -1061$ MeV fm, $V_2 = 400$ MeV fm, $\mu_1 = 0.6$ fm, and $\mu_2 = 1.2$ fm, $r_0 = 1.35$ fm (dotted-dashed lines). (b) Comparison of the real potential of Fig. 1(a) (solid line) with potentials calculated with a δ force (dashed lines) and with Yukawa potentials (dotted-dashed line). The parameters of the potentials fitted on the potential of Fig. 1(a) are given above.

the various inelastic channels.

Restricting the expansion of Q_{2M} in Eq. (10) to the first order terms in $\alpha_{2\mu}$, we have examined three different types of transition potentials $I_2(r)$, which are assumed as real. Then Eq. (10) is simplified:

$$Q_{2M} = I_2(r)(\alpha_{2M}^{(1)} + \alpha_{2M}^{(2)}) . \tag{12}$$

The three different types of coupling potentials $I_2(r)$ are studied in detail in Refs. 22 and 28–30. Here, we only state the main results:

(1) The usual form of the transition potential is obtained by expanding the potential $V(r) = \mathrm{Re}U(r)$ in a Taylor series with respect to multipole deformation coordinates. The result is independent of the L value of the multipole deformation:

$$I_L = -R \frac{dV}{dr} . \tag{13}$$

The potential is depicted in Fig. 2(a). The value of R is about the radius of the colliding nuclei and chosen as $R = 4.25$ fm. Such a potential was initially used in the treatment of α-particle scattering by deformed nuclei[31] and later in the coupled channel calculations for the ^{12}C-^{12}C system by Garvey, Smith, and Hiebert[28] and by Imanishi.[18]

(2) In Ref. 22 a real transition potential was obtained by applying the folding procedure. It was assumed that a δ force of strength V_0 acts between two equal nuclei with homogeneous densities ρ_0 and with surfaces given by Eq. (9). The real and transition potentials result as

$$V(r) = \alpha(1 - r/2R)^2(1 + r/4R) , \tag{14a}$$

$$I_L(r) = \frac{3}{2} \alpha \int_{r/2R}^{1} P_L(x)\,dx \quad (r \leq 2R) \tag{14b}$$

with $\alpha = V_0\rho_0{}^2 4\pi/3R^3$.

Figure 2(a) shows the transition potential I_2 calculated according to Eq. (14b) with the radii $R = 7.5$ and 8.5 fm and the strength $\alpha = -60$ MeV which was obtained by fitting the real potential $V(r)$ in Fig. 1(a) with the potential given in Eq. (14a) [see Fig. 2(b)]. In such a simple procedure we cannot describe Coulomb-nuclear interference effects since the potential (14a) produces only the nuclear part of the nucleus-nucleus interaction.

(3) As discussed in Refs. 22 and 30 and also by Krappe and Nix,[32] analytic expressions for the potentials can be obtained in the folding procedure when homogeneous density distributions are folded with two-body potentials of Yukawa type. In Fig. 2(b) we have fitted the real potential of Fig. 1(a) with a potential in which two two-body potentials of Yukawa type were folded in the homogeneous spherical density distributions of two ^{12}C nuclei with the density $\rho_0 = 3/(4\pi r_0{}^3)$ ($r_0 = 1.35$ fm). The two-body potential has the form:

$$v(\vec{r}_1, \vec{r}_2, \vec{r}) = V_1 \frac{e^{-a/\mu_1}}{a} + V_2 \frac{e^{-a/\mu_2}}{a} ,$$
$$a = |\vec{r}_1 - \vec{r}_2 + \vec{r}| . \tag{15}$$

Here, $\vec{r}_1$ and $\vec{r}_2$ are measured from the centers of the ^{12}C nuclei and $\vec{r}$ is the internuclear separation. The fitted parameters result as $V_1 = -1061$ MeV fm, $V_2 = 400$ MeV fm, $\mu_1 = 0.6$ fm, and $\mu_2 = 1.2$ fm. With this parameter set we calculate the transition potential $I_2(r)$ according to the analytic method outlined in Ref. 22. The resulting coupling potential is shown in Fig. 2(a).

The coupling potentials differ considerably from one another in the interior region. Near the overlapping nuclear surface region the coupling potentials (2) and (3) have a similar radial dependence whereas the potential (1) increases much more steeply.

We use real coupling potentials since the coupling to excited states in heavy ion scattering happens mainly in the touching region of the two nuclei, especially at low bombarding energies, where only a few direct reaction channels are usually open. The ^{12}C-^{12}C scattering is an example

in which there exist very few open direct reaction channels.

IV. ANALYSIS OF THE RESONANCES

In the following we illustrate information about quasimolecular resonances which can be obtained from coupled channel calculations. It is useful to consider the absolute values of the S matrix elements instead of excitation functions in which the effects of resonances are partly averaged out.

In the low energy region ($E_{c.m.} \leq 14$ MeV) with which the present work is primarily concerned, the simultaneous excitation of both target and projectile ^{12}C nuclei is only possible by exciting deep-lying quasibound states in the relative motion, in which case the transmission coefficients are nearly zero. Only smaller effects in the elastic S matrix elements are caused by the simultaneous excitation for $E_{c.m.} \leq 14$ MeV. Therefore, in the present calculations we restrict ourselves to the single excitation of the first 2^+ state at 4.43 MeV in either the ^{12}C target or the ^{12}C projectile.

As pointed out in connection with Eq. (7), four channels have to be coupled for each total angular momentum I. Therefore, the matrix $S^I_{KK'}$ is of dimension 4×4. Using the abbreviation $K=(l,I_1,I_2,J)$ we introduce the square of the S matrix element of the elastic channel as the reflection coefficient

$$\eta_1 = |S^I_{(I000),(I000)}|^2 . \tag{16a}$$

We denote the squares of the transition matrix elements from the elastic channel to the inelastic channels as transition coefficients, defined as

$$\begin{aligned}\eta_2 &= |S^I_{(I000),(l'=I-2,202)}|^2 ,\\ \eta_3 &= |S^I_{(I000),(l'=I,202)}|^2 ,\\ \eta_4 &= |S^I_{(I000),(l'=I+2,202)}|^2 .\end{aligned} \tag{16b}$$

Since the inelastic cross section for the excitation of the 2^+ state is proportional to $\eta_{2,3,4}$, resonances in the transition coefficients lead to resonances in the inelastic excitation function.

A. Reflection coefficient without coupling

Figure 3 presents the reflection coefficient for the optical potential $U(r)$, with the real part as drawn in Fig. 1(a) and the imaginary part as given in Eq. (8) with $W_0=-1.5$ MeV. In the case that the imaginary part is set to zero, the resultant reflection coefficient would be one. Large absorption happens at the position of the resonances of the real potential. Around the resonance energy the relative wave function has a large amplitude inside the potential well which considerably enhances the absorption since the absorption is proportional to the expectation value of the imaginary potential with the relative wave function. Therefore, we fix the position of the resonances ($E_{c.m.} > 5$ MeV) by the minima in the reflection coefficient (see Fig. 3). The resonance energies are listed in Fig. 1(b) and Table I and are distinguished as bound, quasibound, and virtual states according to whether they lie under or above their corresponding Coulomb barriers.

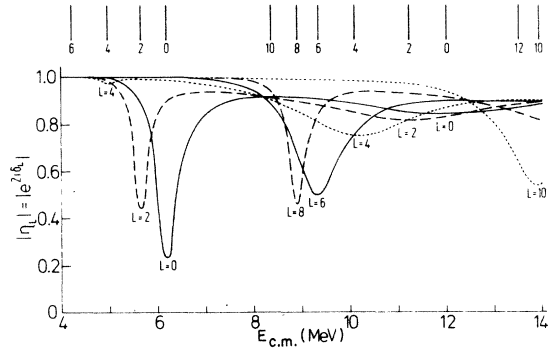

FIG. 3. The reflection coefficients $|\eta_l| = |e^{2i\delta_l}|$. They are computed with the real potential of Fig. 1(a) and the imaginary potential of Eq. (8) with $W_0=-1.5$ MeV. The positions of the potential resonances are drawn above the minima in the reflection coefficients.

Table I and Fig. 1(c) give an overview of the energies and angular momenta of all possible resonances which can be generated from the resonances of the real potential when the single and simultaneous excitations of the first 2^+ state in ^{12}C are coupled to the relative motion. The resonance energies are obtained by adding the excitation energies to the resonance energies of the real potential. They become shifted by the coupling potential which also removes the degeneracy because of its angular momentum dependence.

B. Relation between the reflection and transition coefficients

In Fig. 4 the full set of the coefficients η_i is drawn for the choice of the coupling potential of type 2 with $\alpha=-60$ MeV and $2R=7.5$ fm. The strength of the imaginary potential is set equal to $W_0=-1.5$ MeV in all channels. In Table II we compare the minima in the reflection coefficient and the maxima in the transition coefficients with the unshifted resonances of Table I and Fig. 1(c). The correspondence between the unshifted resonances and the maxima in the transition coefficients can easily be resolved because the total and orbital angular momentum of the maxima are known for each transition coefficient. On the contrary the minima in the reflection coefficient are specified

TABLE I. Position of the unshifted resonances in the ^{12}C-^{12}C system. The first two columns give the energy and angular momenta of the resonances of the ^{12}C-^{12}C system where the ^{12}C nuclei are in the ground state (g.s.) or one of the ^{12}C nuclei or both are excited to the first 2^+ state at 4.43 MeV. In the third and fourth columns we have listed the energy and state of the intrinsic excitation of the ^{12}C nuclei. The last three columns state the energy, angular momentum, and type of the resonance in the radial motion of the nuclei (B = bound, QB = quasibound, V = virtual). The energies of the $^{12}C + ^{12}C$ resonances in column 1 are obtained by adding columns 3 and 5. The angular momenta in column 2 result by vector addition of the angular momentum in column 6 and of the angular momentum of the intrinsic excitation of the ^{12}C nuclei. The resonance states are depicted in Figs. 1(b) and 1(c).

Position of the resonance		Intrinsic excitation of the $^{12}C + ^{12}C$ system		Excited bound, quasibound, and virtual state of the $^{12}C + ^{12}C$ potential		
Energy (MeV)	Angular momentum	Excitation energy	State	Energy (MeV)	Angular momentum	State
4.08	6	0	g.s. + g.s.	4.08	6	QB
4.27	0, 2, 4, 6	8.86	$2^+ + 2^+$	−4.59	2	B
4.95	4	0	g.s. + g.s.	4.95	4	QB
5.03	0, 2, 4	4.43	g.s. + 2^+	0.60	2	QB
5.66	0, 2, 4	8.86	$2^+ + 2^+$	−3.20	0	B
5.68	2	0	g.s. + g.s.	5.68	2	QB
6.01	2	4.43	g.s. + 2^+	1.58	0	QB
6.27	0	0	g.s. + g.s.	6.27	0	QB
7.26	2, 4, 6, 8, 10	8.86	$2^+ + 2^+$	−1.60	6	B
7.63	6, 8, 10	4.43	g.s. + 2^+	3.20	8	QB
8.30	10	0	g.s. + g.s.	8.30	10	QB
8.34	0, 2, 4, 6, 8	8.86	$2^+ + 2^+$	−0.52	4	B
8.51	4, 6, 8	4.43	g.s. + 2^+	4.08	6	QB
8.89	8	0	g.s. + g.s.	8.89	8	QB
9.34	6	0	g.s. + g.s.	9.34	6	V
9.38	2, 4, 6	4.43	g.s. + 2^+	4.95	4	QB
9.46	0, 2, 4, 6	8.86	$2^+ + 2^+$	0.60	2	QB
10.11	0, 2, 4	4.43	g.s. + 2^+	5.68	2	QB
10.18	4	0	g.s. + g.s.	10.18	4	V
10.44	0, 2, 4	8.86	$2^+ + 2^+$	1.58	0	QB
10.70	2	4.43	g.s. + 2^+	6.27	0	QB
11.22	2	0	g.s. + g.s.	11.22	2	V
12.00	0	0	g.s. + g.s.	12.00	0	V
12.06	4, 6, 8, 10, 12	8.86	$2^+ + 2^+$	3.20	8	QB
12.73	8, 10, 12	4.43	g.s. + 2^+	8.30	10	QB
12.94	2, 4, 6, 8, 10	8.86	$2^+ + 2^+$	4.08	6	QB
13.32	6, 8, 10	4.43	g.s. + 2^+	8.89	8	QB
13.50	12	0	g.s. + g.s.	13.50	12	QB
13.77	4, 6, 8	4.43	g.s. + 2^+	9.34	6	V
13.81	0, 2, 4, 6, 8	8.86	$2^+ + 2^+$	4.95	4	QB
13.91	10	0	g.s. + g.s.	13.91	10	V

only by the total angular momentum and, therefore, no unique classification of the minima can be reached unless the transition coefficients are analyzed.

The results shown in Fig. 4 are an illustrative example for the double resonance mechanism suggested in Ref. 19. The double resonance mechanism explains the enhancement of certain transition coefficients by the effect that for certain energies and total angular momenta a virtual orbital state in the elastic channel and a quasibound state in an inelastic channel are simultaneously resonating. Quasibound states can only be excited with sufficient strength if the feeding partial wave of the elastic channel has an enhanced amplitude inside the potential well. This condition is fulfilled for elastic partial waves which resonate, in addition, with a virtual state of the molecular-type real potential. For the appearance of the double resonance effect it is necessary that the difference in energy and angular momentum between the resonating virtual and quasibound orbital states can be matched with the excitation energy and angular momentum of the intrinsic nuclear states, i.e.,

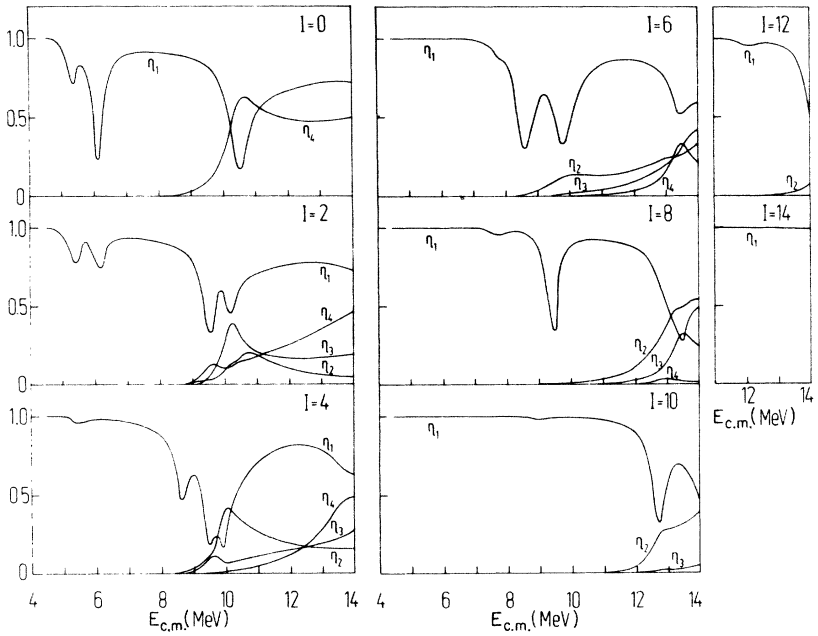

FIG. 4. The reflection coefficients η_1 and the transition coefficients $\eta_{2,3,4}$ as defined in Eqs. (16a) and (16b). The transition coefficients $\eta_{2,3,4}$ belong to the transitions from the elastic channel to the excited channels with $l = I - 2, I, I+2$, respectively. The coupling potential used is of type 2 with $\alpha = -60$ MeV and $2R = 7.5$ fm and is depicted in Fig. 2(a). The strength of the imaginary potential is set equal to $W_0 = -1.5$ MeV in all channels.

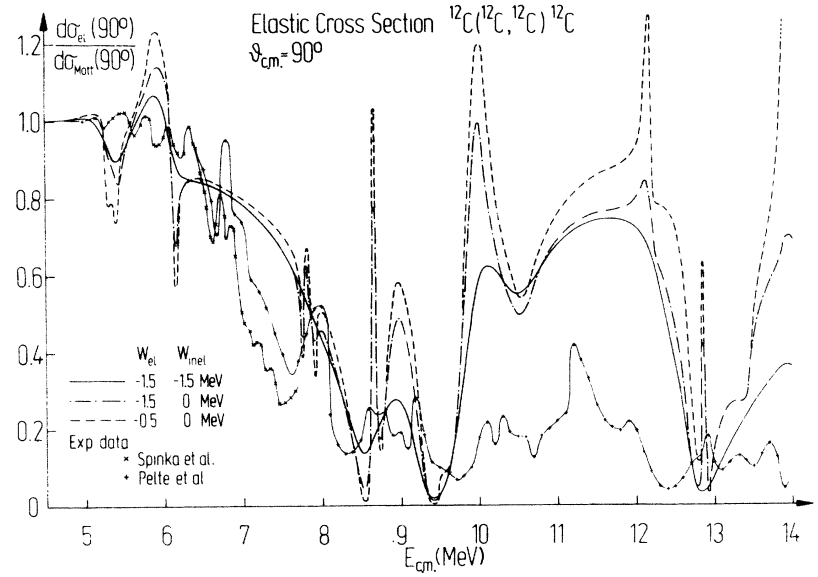

FIG. 5. The elastic excitation function $(d\sigma_{el}/d\Omega)/(d\sigma_{Mott}/d\Omega)$ at $\vartheta_{c.m.} = 90°$ for ^{12}C-^{12}C scattering. The experimental data are represented by the crosses and are taken from Ref. 7 for $E_{c.m.} \lesssim 7.5$ MeV and from Ref. 34 for $E_{c.m.} \gtrsim 6.5$ MeV. The theoretical excitation functions are computed with the type 2 coupling potential with $\alpha = -60$ MeV and $2R = 8.5$ fm for various strengths W_0 of the imaginary potential. The following choices are made: (i) $W_0 = -1.5$ MeV in the elastic and inelastic channels (solid line); (ii) $W_0 = W_{el} = -1.5$ MeV in the elastic and $W_0 = W_{inel} = 0$ in the inelastic channels (dotted-dashed line); (iii) $W_{el} = -0.5$ and $W_{inel} = 0$ (dashed line).

TABLE II. Comparison of the experimental resonances (columns 1–3), the unshifted resonances for no coupling and the single excitation of Table I (columns 4 and 5), the resonances in the reflection and transition coefficients depicted in Fig. 4 (columns 6,7), and the energies of the maxima in the 90° differential cross section for the inelastic excitation of the first 2^+ state in ^{12}C (columns 8–10). The sources of the experimental data are indicated in column 3. The numbers in parentheses behind the energies of the unshifted resonances and the resonances in the reflection and transition coefficients are the total angular momenta I of each resonance state. The [illegible]cients are additionally marked by the angular momentum l of the corresponding orbital resonance. The energies of the maxima in the inela[illegible] function are obtained from Fig. 6. The experimental maxima are taken from Ref. 34. All energies are given in MeV.

Exp. resonances			Unshifted resonances		Resonances in η_i		Energies of maxima in $d\sigma(2^+, 90°)/d\Omega$		
			No coupling	2^+ coupling	η_1	η_2, η_3, η_4		Calculated	
E_{res}	I^π_{res}	Ref.	$E_{res}(I)$	$E_{res}(I)$	$E_{res}(I)$	$E_{res}(l, I)$	Exp.	$W_{el} = W_{inel} = -1,5$ MeV	$W_{el} = -1,5$ MeV, $W_{inel} = 0$
4.03		7	4.08 (6)						
4.22 }	4^+	7							
4.25 }	0^+	11							
4.44	$4^+(2^+)$	7,11							
4.58	2^+	7,11							
4.86	$4^+, 2^+$	7,11							
4.98	2^+	7,11	4.95 (4)	5.03 (0,2,4)					
5.23		7							
					5.35 (2)				
					5.40 (0)				
					5.45 (4)				
5.62	2^+	7	5.68 (2)						
5.98	4^+	7		6.01 (2)	6.10 (0)				
					6.15 (2)				
6.28	$(0^+), 2^+$	7,11	6.27 (0)						
7.50	6^+	9							
				7.63 (6,8,10)					
7.71	4^+	8			7.75 (8)				
					7.80 (6)				
8.45	6^+	9	8.30 (10)						
				8.51 (4,6,8)					
					8.60 (6)				
					8.65 (4)				8.65
8.85	8^+	9	8.89 (8)						
								8.80	8.85
					9.0 (10)				

TABLE II. (*Continued*)

Exp. resonances			Unshifted resonances		Resonances in η_i		Energies of maxima in $d\sigma(2^+, 90°)/d\Omega$		
			No coupling	2^+ coupling	η_1	η_2, η_3, η_4		Calculated	
E_{res}	I^π_{res}	Ref.	$E_{res}(I)$	$E_{res}(I)$	$E_{res}(I)$	$E_{res}(l, I)$	Exp.	$W_{el} = W_{inel} = -1,5$ MeV	$W_{el} = -1,5$ MeV, $W_{inel} = 0$
9.25		9	9.34 (6)						
				9.38 (2,4,6)					
					9.48 (4)				
					9.50 (8)				9.50
					9.55 (2)	9.65 (4,2)			
					9.75 (6)	9.65 (4,4)			
9.84	8^+	8			9.93 (4)		9.8		
				10.11 (0,2,4)		10.05 (2,4)			
			10.18 (4)			10.10 (4,6)			10.18
					10.20 (2)	10.25 (2,2)	10.35	10.35	10.35
					10.50 (0)	10.65 (2,0)			
							10.7		
				10.70 (2)		10.80 (0,2)			
11.2	8^+	9					11.0		
			11.22 (2)						
11.43	8^+	13					11.3		
(11.78)	8^+	13							
							11.8		
			12.00 (0)						
12.0	8^+	13			12.10 (12)				
12.35	8^+	13							
					12.70 (10)				
12.86	8^+	13		12.73 (8,10,12)		12.90 (8,10)			
						12.90 (10,10)	12.8		12.90
13.35	10^+	13		13.32 (6,8,10)		12.95 (10,8)	13.1		
					13.45 (6)	13.45 (8,6)			13.43
			13.50 (12)		13.50 (8)	13.55 (8,8)		13.50	
13.8	10^+	9		13.77 (4,6,8)					
13.85	10^+	13	13.91 (10)		~14 (10)	~14 (6,4)	14.0		
					~14 (12)	~14 (6,6)			
						~14 (6,8)			

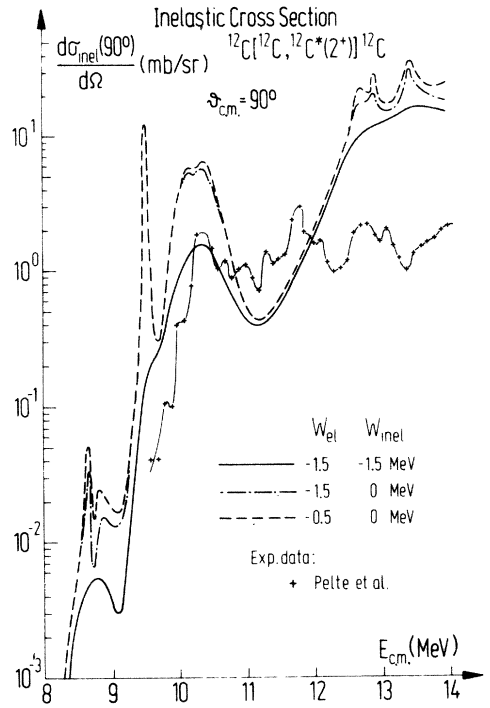

FIG. 6. The 90° differential cross section for the excitation of the first 2^+ state in the ^{12}C-^{12}C scattering. The experimental data are represented by the crosses and taken from Ref. 34. The theoretical cross sections are computed with the same choices of parameters as used for the elastic excitation function in Fig. 5. The following strengths W_0 of the imaginary potential are chosen: (i) $W_{el}=W_{inel}=-1.5$ MeV (solid line); (ii) $W_{el}=-1.5$ MeV, $W_{inel}=0$ (dotted-dashed line); (iii) $W_{el}=-0.5$ MeV, $W_{inel}=0$ (dashed line).

of the 2^+ (4.43 MeV) state of ^{12}C in our calculations.

In the investigated energy range between 5 and 14 MeV three distinguishable groups of molecular states in the elastic channel lead to double resonance effects, namely the states [see Figs. 1(b), 1(c), and Table I]:

1. $I=2,0$ at 5.68, 6.27 MeV;

2. $I=6,4,2,0$ at 9.34, 10.18, 11.22, 12.00 MeV;

3. $I=10,8,6$ at 13.91, 14.70, 16.18 MeV.

These three groups can be clearly observed in Figs. 3 and 4. The first group around 6 MeV shows effects in the reflection coefficients only since the relative kinetic energy in the inelastic channels is too low to permit an appreciable amount of the flux to tunnel through the barriers. Although the orbital states of group 1 are quasibound, their widths are wide enough (see Fig. 3) to overlap with inelastic resonance states.

The largest effects in the reflection and transition coefficients are produced by the elastic partial waves resonating with the virtual states of group 2. A wide valley appears in the reflection coefficient between 8 and 11 MeV in which the inelastic resonances are embedded. Analyzing the transition coefficients we find that the states of group 1 are most strongly excited in the inelastic channels between 10 and 11 MeV. As shown in Figs. 1(b) and 1(c) the energy difference between two following molecular states with the same angular momentum is of the order of 5–6 MeV, and, therefore, the ^{12}C excitation energy of 4.43 MeV matches the energy difference for a double resonance event in all cases where the orbital states in the elastic channel have a width of about 1–2 MeV.

The same effects as discussed for the states of group 2 are repeated in the energy range between 13 and 16 MeV by the orbital states of group 3 acting as doorway states for inelastic excitations. The molecular states excited in the inelastic channels are the states of group 2 and, in addition, the state with $I=8$ at 8.89 MeV. Since the states of group 2 already lie above their corresponding

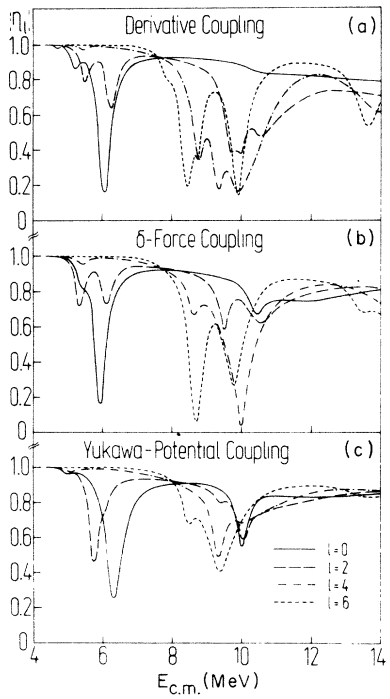

FIG. 7. Dependence of the reflection coefficients $|\eta_l|$ on the type of the coupling potential. The strength of the imaginary potential is chosen as $W_0=-1.5$ MeV in all channels. The coupling potentials are (a) the derivative type; (b) the δ-force type with $\alpha=-60$ MeV, $2R=8.5$ fm; (c) the Yukawa-potential type with $V_1=-1061$ MeV fm, $\mu_1=0.6$ fm, $V_2=400$ MeV fm, $\mu_2=1.2$ fm. The coupling potentials are depicted in Fig. 2(a).

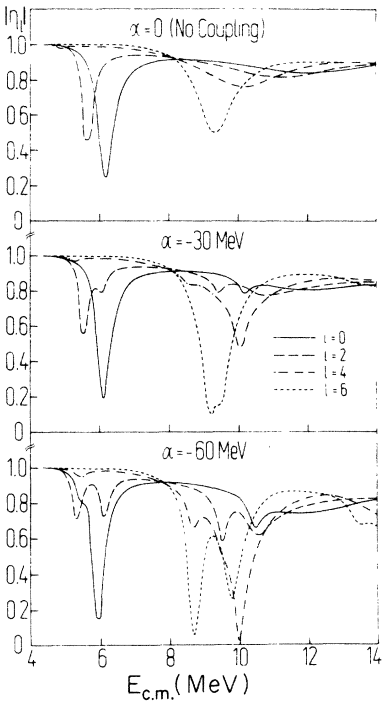

FIG. 8. Dependence of the reflection coefficients $|\eta_l|$ on the strength α of the coupling potential of type 2. The parameters are $2R = 8.5$ fm and $W_0 = -1.5$ MeV in all channels. With growing coupling strength the resonance minima become more prominent.

barriers, the peaks in the transition coefficients are broadened more than at lower energies.

In Figs. 5 and 6 the elastic and inelastic 90° cross sections are presented for various choices of the strength W_0 of the imaginary potential in the elastic and inelastic channels. In Fig. 5 one notes three distinguishable groups of resonances around 6, 8–10, and 12–14 MeV. With the increasing strength of the imaginary potential the resonances get smeared out. The inelastic cross section in Fig. 6 reveals the resonance structures in the transition coefficients around 10 and 13–14 MeV. In Table II we have listed the resonances in the inelastic 90° cross section obtained with the coupled channel calculations.

From Figs. 5 and 6 it becomes obvious that the resonance structures of the cross sections are sensitively influenced by the strength of the imaginary potential (see also Fig. 9).

C. Dependence of the reflection coefficient on the coupling and imaginary potential

In this section we discuss the dependence of the reflection coefficient on various parameters. In all the examples presented in the following the same strength W_0 of the imaginary potential is used for the elastic and inelastic channels.

1. Dependence on the shape of the coupling potential

In Fig. 7 the reflection coefficients are drawn for the three different choices of the coupling potentials discussed in Sec. III B and shown in Fig. 2(a). The coupling potential of type 1 produces the largest coupling effects, since the strength of this potential is the largest of the coupling potentials considered, which is obvious from Fig. 2(a). The different radial shapes of the coupling potentials are responsible for the resonances being differently exhibited in the reflection coefficients. We note also that the positions of the resonances are slightly shifted for different coupling potentials.

2. Dependence on the strength of the coupling potential

Figure 8 shows the variation of the reflection coefficient as a function of the coupling strength α for the coupling potential of type 2. The case of no coupling ($\alpha = 0$) is also depicted in Fig. 3. Two effects should be remarked: With increasing

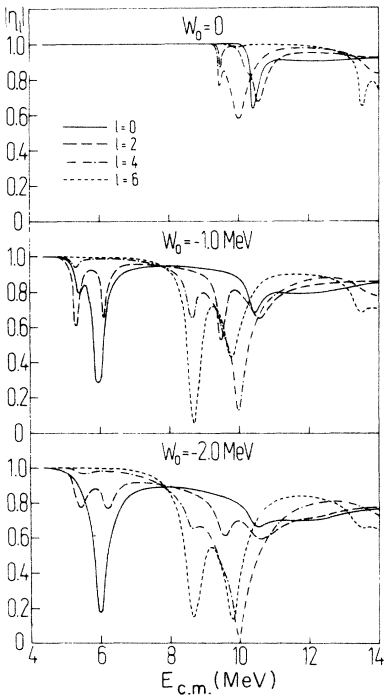

FIG. 9. Dependence of the reflection coefficients $|\eta_l|$ on the strength of the imaginary potential $W_0 = W_{el} = W_{inel}$ which is chosen the same in all channels. The coupling potential is of type 2 with $\alpha = -60$ MeV and $2R = 8.5$ fm. In the case of $W_0 = 0$ the absorption in the reflection coefficient is solely caused by the coupling of the first 2^+ state in ^{12}C.

coupling strength the resonances become more and more prominent and the positions of the resonances are shifted.

3. Dependence on the strength of the imaginary potential

In Fig. 9 the strength of the imaginary potential is varied. Since the imaginary potential is surface-peaked, and the quasimolecular resonances are localized more inside the potential well, the imaginary potential used does not destroy the resonance structure in the reflection coefficients. The imaginary potential is weakly absorbing, as can be recognized by the reflection coefficients in Fig. 3 which do not deviate much from one in the energy range between 10 and 14 MeV. Volume-absorbing imaginary potentials lead to reflection coefficients which fall above 15 MeV to zero as shown in Ref. 22. The curves for the zero imaginary potential in Fig. 9 clearly reveal the absorption in the elastic channel which is caused by the direct coupling of the inelastic continuum channels.

V. RESULTS AND CONCLUSIONS

Many of the resonances observed in the ^{12}C-^{12}C system can be interpreted as single particle shape resonances in an effective ^{12}C-^{12}C potential. In Table II we have listed the experimental resonances observed in various reactions: the measurement of the γ yield of the ^{12}C-^{12}C reaction by Spinka *et al.*[7]; the $^{12}C(^{12}C,\alpha)^{20}Ne^*$ reaction populating low-lying levels of ^{20}Ne by Erb *et al.*,[8] Basrak *et al.*,[9] and Voit *et al.*[11]; the $^{12}C(^{12}C,p)^{23}Na^*$ reaction by Basrak *et al.*[9]; and the measurement of the $^{8}Be + {}^{16}O$ exit channel by Fletcher *et al.*[13] and Eberhardt *et al.*[14] Comparing the calculated resonances in the reflection coefficient and their angular momenta with the experimental resonances we conclude that the applied quasimolecular potential and the coupling of the first 2^+ state of ^{12}C are sufficient to give a semiquantitative explanation of the observed resonances.

It should be noted that the positions of the resonances depend quite sensitively on the real potential and excitation energies of the ^{12}C nucleus. The positions are nearly unaffected by special assumptions about the imaginary potential and the coupling potentials. Therefore, a classification of the observed resonances in terms of the molecular resonances fixes, with some accuracy, the shape of the real potential. For a quantitative comparison with experiment α-transfer channels and channels to higher excited states in ^{12}C also have to be coupled into the investigated channels.

A systematic study of the energy dependence of the reflection and transition coefficients and their dependence on the coupling and imaginary potential are useful in the determination of the character of the resonances in the calculated cross sections. The widths and shapes of the resonances in the reflection and transition coefficients are not yet directly comparable with experimental data. But extended phase shift analyses of the experimental data for various reaction channels as done for the elastic ^{12}C-^{12}C and ^{16}O-^{16}O scattering by Voit and Helb[33] would be a valuable tool for obtaining more precise data about the resonances, which may be directly used for comparison with coupled channel calculations.

In Figs. 5 and 6 we compare the calculated elastic and inelastic ^{12}C-^{12}C cross sections for $\vartheta_{c.m.} = 90^\circ$ with the experimental data of Spinka *et al.*[7] and Pelte *et al.*[34] Whereas the reflection coefficients always reveal finer resonance structures, the resonance structures become partly smeared out with an increasing imaginary potential in the calculated cross sections. Intermediate resonance structures in the experimental cross sections have two different origins: They may be caused by compound elastic statistical fluctuations[35] or by inelastic excitations and α-transfer reactions which both couple very strongly to the elastic channels. In the ^{12}C-^{12}C system most of the intermediate structure, especially the resonance structure near the Coulomb barrier, is of nonstatistical origin. The appearance of intermediate structure in the ^{12}C-^{12}C system is closely linked with the surface transparency of the grazing partial waves. The surface transparency is caused by the fact that grazing partial waves have only a small overlap with the compound states of the amalgamated ^{24}Mg system.[22,25] Therefore, a more accurate imaginary potential depends on the total angular momentum of the system and lets the grazing partial waves remain unabsorbed. The unabsorbed partial waves generate the gross structures in the cross sections and play the role of doorway states for the double resonance mechanism in which intermediate structure is produced.[25]

To obtain a more quantitative agreement between the measured and calculated cross sections three nontrivial improvements have to be considered: (a) The angular momentum and energy dependence of the imaginary potential has to be improved in the framework of the theories worked out in Refs. 22 and 25. The imaginary potential is the key for the understanding of the appearance of gross and intermediate structures. (b) The direct and coupling potentials have to be consistently calculated in the adiabatic approximation by use of the two-center shell model and the Strutinsky-renormalization procedure.[26] (c) The α-transfer channel has to be coupled to the elastic

channel. This last problem is numerically difficult to handle since the α transfer generates nonlocal transition potentials caused by recoil and nonorthogonality effects.[36]

It may be noted that our interpretation of the resonance structures in the cross sections as resonance states in the quasimolecular potential depends on whether a double resonance excitation is possible or not. The double resonance mechanism leads to effects which have sufficient strength to give rise to intermediate structures in the cross sections. The discussion of the reflection and transition coefficients in Sec. IV shows the importance of the double resonance mechanism in generating intermediate structures.

ACKNOWLEDGMENT

We thank Dr. Hans Joachim Fink for fruitful discussions and for his aid in the computer programs. Discussions with Professor Mosel and Professor Cindro are gratefully acknowledged.

---

*Work supported by the Bundesministerium für Forschung und Technologie, by the Gesellschaft für Schwerionenforschung, and by the Deutsche Forschungsgemeinschaft.

[1]D. A. Bromley, J. A. Kuehner, and E. Almqvist, Phys. Rev. Lett. 4, 365 (1960); Phys. Rev. 123, 878 (1961); E. Almqvist, D. A. Bromley, and J. A. Kuehner, Phys. Rev. Lett. 4, 515 (1960).

[2]D. A. Bromley, in Proceedings of the Second International Conference on Clustering Phenomena in Nuclei, 1975, Univ. of Maryland (unpublished), ERDA Report No. ORO-4856-26, p. 465.

[3]E. W. Vogt and H. McManus, Phys. Rev. Lett. 4, 518 (1960).

[4]R. H. Davis, Phys. Rev. Lett. 4, 521 (1960).

[5]J. R. Patterson, H. Winkler, and C. S. Zaidens, Astrophys. J. 157, 367 (1969); J. R. Patterson, B. N. Nagorcka, G. D. Symons, and W. M. Zuk, Nucl. Phys. A165, 545 (1971).

[6]M. G. Mazarakis and W. E. Stephens, Phys. Rev. C 7, 1280 (1973); Astrophys. J. 171, L97 (1972).

[7]H. Spinka, Ph.D. thesis, California Institute of Technology, 1971 (unpublished); H. Spinka and H. Winkler, Astrophys. J. 174, 455 (1972); Nucl. Phys. A233, 456 (1974).

[8]K. A. Erb, R. R. Betts, D. L. Hanson, M. W. Sachs, R. L. White, P. P. Tung, and D. A. Bromley, Phys. Rev. Lett. 37, 670 (1976).

[9]Z. Basrak, F. Auger, B. Fernandez, J. Gastebois, and N. Cindro, Lett. J. Phys. (Paris) 37, L131 (1976); Phys. Lett. 65B, 119 (1976); N. Cindro *et al.* (unpublished).

[10]H. Voit, P. Dück, W. Galster, E. Haindl, G. Hartmann, H. D. Helb, F. Siller, and G. Ischenko, Phys. Rev. C 10, 1331 (1974); H. Voit, G. Ischenko, and F. Siller, Phys. Rev. Lett. 30, 564 (1973).

[11]W. Galster, W. Treu, P. Dück, H. Fröhlich, and H. Voit, Phys. Rev. C 15, 950 (1977).

[12]E. R. Cosman, T. M. Cormier, K. van Bibber, A. Sperduto, G. Young, I. Erskine, L. R. Greenwood, and O. Hansen, Phys. Rev. Lett. 35, 265 (1975).

[13]N. R. Fletcher, J. D. Fox, G. J. KeKelis, G. R. Morgan, and G. A. Norton, Phys. Rev. C 13, 1173 (1976).

[14]K. A. Eberhard, E. Mathiak, J. Stettmeier, W. Trombik, A. Weidinger, L. N. Wuestefeld, and K. G. Bernhardt, Phys. Lett. 56B, 445 (1975); in Proceedings of the Second International Conference on Clustering Phenomena in Nuclei, 1975 (see Ref. 2), p. 530.

[15]N. Cindro, in *Nuclear Spectroscopy and Nuclear Reactions with Heavy Ions*, Proceedings of the International School of Physics "Enrico Fermi," Course LXII, edited by H. Faraggi and R. A. Ricci (North-Holland, Amsterdam, 1976), p. 271; Proceedings of the Fifteenth International Winter School on Nuclear Spectroscopy, Zakopane, Poland, 1977 (unpublished).

[16]H. Feshbach, in *Proceedings of the European Conference on Nuclear Physics with Heavy Ions, Caen, 1976* [J. Phys. (Paris) 37, C5-177 (1976)].

[17]A. Richter and C. Toepffer, Institut für Kernphysik, TH Darmstadt, Report No. IKDA 77/3, 1977 (unpublished).

[18]B. Imanishi, Phys. Lett. 27B, 267 (1968); Nucl. Phys. A125, 33 (1969).

[19]W. Scheid, W. Greiner, and R. Lemmer, Phys. Rev. Lett. 25, 176 (1970).

[20]J. Y. Park, W. Scheid, and W. Greiner, Phys. Rev. C 10, 967 (1974).

[21]B. N. Nagorcka and J. O. Newton, Phys. Lett. 41B, 34 (1972).

[22]H. J. Fink, W. Scheid, and W. Greiner, Nucl. Phys. A188, 259 (1972).

[23]Y. Kondo, T. Matsuse, and Y. Abe, in *Proceedings of the Second International Conference on Clustering Phenomena in Nuclei, 1975* (see Ref. 2), p. 532; Y. Abe, *ibid.*, p. 500.

[24]O. Tanimura, Tokyo University Institute for Nuclear Studies Report No. INS-267, Tokyo, 1976 (unpublished).

[25]W. Greiner and W. Scheid, J. Phys. (Paris) 32, C6-91 (1971); H. J. Fink, H. Müller, and W. Scheid, in *Proceedings of the Europhysics Study Conference on Intermediate Processes in Nuclear Reactions, Plitvice, Yugoslavia*, edited by N. Cindro, P. Kulišić, and T. Mayer-Kuckuk (Springer-Verlag, Berlin, 1973), in *Lecture Notes in Physics* (Springer-Verlag, Berlin, 1973), Vol. 22, p. 144.

[26]H. J. Fink, W. Scheid, and W. Greiner, J. Phys. G 1, 685 (1975).

[27]S. J. Skorka, J. Hertel, and T. W. Retz-Schmidt, Nucl. Data A2, 369 (1966).

[28]G. T. Garvey, A. M. Smith, and J. C. Hiebert, Phys. Rev. 130, 2397 (1963).

[29]R. H. Bassel, G. R. Satchler, and R. M. Drisko, Nucl. Phys. 89, 419 (1966).

[30]V. Oberacker, H. Holm, and W. Scheid, Phys. Rev. C 10, 1917 (1974).

[31]R. H. Bassel, G. R. Satchler, R. M. Drisko, and E. Rost, Phys. Rev. 128, 2693 (1962); E. Rost, *ibid.*

128, 2708 (1962).
[32]H. J. Krappe and J. R. Nix, in *Proceedings of the International Atomic Energy Agency Symposium on the Physics and Chemistry of Fission, Rochester, 1973* (IAEA, Vienna, 1974), Vol. I, p. 159.
[33]H. Voit and H. D. Helb, Nucl. Phys. A204, 196 (1973).
[34]H. Emling, R. Nowotny, D. Pelte, and G. Schrieder, Nucl. Phys. A211, 600 (1973); H. Emling, R. Nowotny, D. Pelte, G. Schrieder, and W. Weidenmeier, *ibid.* A239, 172 (1975).
[35]E. Almqvist, J. A. Kuehner, D. Mc Pherson, and E. W. Vogt, Phys. Rev. 136, B84, B99 (1964).
[36]O. Krause, Ph.D. thesis, University Frankfurt, 1976 (unpublished).
[37]Further references for resonances at energies above $E_{c.m.}$=14 MeV: H. T. Fortune, T. H. Braid, R. E. Segel, and K. Raghunathan, Phys. Lett. 63B, 403 (1976); H. T. Fortune, S. C. Headley, L. R. Medsker, T. H. Braid, R. E. Segel, and K. Raghunathan, Phys. Rev. C14, 1271 (1976); T. M. Cormier *et al.*, Phys. Rev. Lett. 38, 940 (1977).